

Clock-Line-Mediated Sisyphus Cooling

Chun-Chia Chen (陳俊嘉)^{1,2,*}, Jacob L. Siegel^{1,2,*}, Benjamin D. Hunt^{1,2}, Tanner Grogan,^{1,2} Youssef S. Hassan^{1,2},
 Kyle Beloy¹, Kurt Gibble^{1,3}, Roger C. Brown¹ and Andrew D. Ludlow^{1,2,‡}

¹*National Institute of Standards and Technology, 325 Broadway, Boulder, Colorado 80305, USA*

²*University of Colorado, Department of Physics, Boulder, Colorado 80309, USA*

³*Department of Physics, The Pennsylvania State University, University Park, Pennsylvania 16802, USA*

 (Received 3 December 2023; revised 9 March 2024; accepted 18 June 2024; published 31 July 2024)

We demonstrate subrecoil Sisyphus cooling using the long-lived 3P_0 clock state in alkaline-earth-like ytterbium. A 1388-nm optical standing wave nearly resonant with the $^3P_0 \rightarrow ^3D_1$ transition creates a spatially periodic light shift of the 3P_0 clock state. Following excitation on the ultranarrow clock transition, we observe Sisyphus cooling in this potential, as the light shift is correlated with excitation to 3D_1 and subsequent spontaneous decay to the 1S_0 ground state. We observe that cooling enhances the loading efficiency of atoms into a 759-nm magic-wavelength one-dimensional (1D) optical lattice, as compared to standard Doppler cooling on the $^1S_0 \rightarrow ^3P_1$ transition. Sisyphus cooling yields temperatures below 200 nK in the weakly confined, transverse dimensions of the 1D optical lattice. These lower temperatures improve optical lattice clocks by facilitating the use of shallow lattices with reduced light shifts while retaining large atom numbers to reduce the quantum projection noise. This Sisyphus cooling can be pulsed or continuous and is applicable to a range of quantum metrology applications.

DOI: [10.1103/PhysRevLett.133.053401](https://doi.org/10.1103/PhysRevLett.133.053401)

Laser cooling the motion of atoms and molecules enables exquisite quantum control of both their internal and external degrees of freedom. Their rich multilevel structure can be a powerful platform for quantum sensors [1], quantum simulation [2], and information encoding through quantum control [3–5], as well as precision measurements for tests of fundamental physics [6].

As the motivation to exploit more diverse quantum systems has grown, so have the efforts to cool these species. For example, laser cooling of antihydrogen has significantly improved the spectroscopy of antimatter, advancing tests of charge-parity-time invariance [7]. Remarkable progress has also been made in the field of molecule laser cooling, specifically in the efficient cooling of molecules with nearly-diagonal Franck-Condon factors [8] and those possessing optical cycling centers [9,10]. Beyond cooling more species, the drive for improved quantum control has also motivated deeper cooling techniques. For example, the finite temperature of optical-tweezer-trapped atoms causes random Doppler shifts and position fluctuations, thereby imposing additional constraints on entanglement generation and lifetime [4]. For optical lattice clocks that utilize alkaline-earth(-like) elements, extremely low temperatures can facilitate shallow lattices, which is key to realizing fractional frequency

uncertainty at 10^{-18} or below [11–13]. Furthermore, the metastable states in these elements are well suited not just for next-generation optical atomic clocks, but also for long-lived entangled qubits [14,15] and atom interferometry [16]. In these cases, the combination of a strong cycling transition and weaker intercombination transition are ideally used to reach atomic temperatures approaching the μK level, though deeper cooling is advantageous. This is especially true for alkaline-earth(-like) atoms where the intercombination linewidth is either too narrow or too broad to usefully reach μK temperatures, with Mg (36 Hz) [17] and Hg (1.3 MHz) [18] being extreme examples of this.

Here, we adapt a cooling technique proposed for (anti) hydrogen [19,20] to the alkaline-earth-like species ytterbium. The cooling uses an excited-state Sisyphus potential created with a spatially varying ac-Stark-shifting-laser blue detuned to the $^3P_0 \rightarrow ^3D_1$ transition. To cool, an ultranarrow clock laser excites atoms from the virtually unperturbed 1S_0 ground state to the bottom of the 3P_0 Sisyphus potential; see Fig. 1(a). After atoms lose kinetic energy by climbing the Sisyphus potential, they preferentially absorb $^3P_0 \rightarrow ^3D_1$ photons at places away from the potential's minimum due to the higher intensity of the blue-detuned ac-Stark-shifting laser. Atoms then spontaneously decay to the 1S_0 state, completing a cooling cycle. By adjusting the Rabi frequency of the clock excitation, we can optimize the technique to achieve either faster cooling or lower temperatures.

*These authors contributed equally to this letter.

†Contact author: chenchunchia@gmail.com

‡Contact author: andrew.ludlow@nist.gov

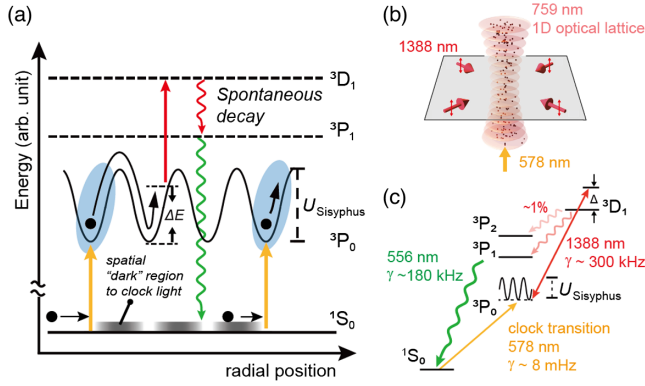


FIG. 1. Clock-line-mediated Sisyphus cooling. (a) Laser light resonant with the $^1S_0 \rightarrow ^3P_0$ clock transition excites atoms near the minima of the spatially varying energy of the 3P_0 state. Atoms then traverse the Sisyphus potential with a depth of U_{Sisyphus} before absorbing a $^3P_0 \rightarrow ^3D_1$ photon. Excitation to the 3D_1 state is followed by spontaneous decay to the ground state, by way of the 3P_1 state, completing a Sisyphus cycle with a ΔE energy dissipation. (b) Two pairs of counterpropagating 1388-nm beams cross orthogonally and form a 2D standing wave in the transverse plane of the 1D optical lattice. The 578-nm clock-excitation laser is aligned along the longitudinal axis of the 1D 759-nm magic-wavelength lattice. (c) Simplified Yb level diagram and transitions used in the Sisyphus cooling. A quasiclosed Sisyphus-cooling cycle is established with $\sim 1\%$ branching to the 3P_2 state.

Tuning the Stark-shifting laser closer to resonance to increase the Sisyphus potential depth, we cool the atomic sample prepared from the $^1S_0 - ^3P_1$ narrow-line magneto-optical trap (MOT). Doing so enhances the number of cold atoms that can be loaded into a 1D magic-wavelength optical lattice [21] by a factor of 4. By then implementing 1D Sisyphus cooling on atoms trapped in the lattice, we achieve cooling temperatures below 200 nK along a weakly confined axis of the lattice. Instead, with a 2D Sisyphus potential in the radial plane of the 1D optical lattice, we demonstrate 3D cooling, achieving both recoil-limited temperatures along the radial axes as well as cooling along the lattice axis. We further combine Sisyphus cooling with energy-selective excitation on the clock transition tuned to a lattice motional sideband. This technique, similar to cyclic cooling [22], reduces the trapped atomic sample's energy distribution along the weak confinement axis. Because the Sisyphus-cooling scheme utilizes the narrow-band clock line shared by alkaline-earth(-like) systems, the technique may readily be applied to elements such as Cd, Hg, Mg, and Ra, which have otherwise less favorable Doppler cooling properties [18,23–25].

Our apparatus and the experimental details to prepare ultracold Yb loaded into a 1D 759-nm magic-wavelength lattice have been described elsewhere [26]. Here, we take laser cooling on the 556-nm $^1S_0 - ^3P_1$ intercombination transition as our initial condition. We introduce two pairs of counterpropagating 1388-nm beams that cross

orthogonally and are located in the plane perpendicular to the magic-wavelength lattice axis; see Fig. 1(b). The 1388-nm laser beams are collimated, with ~ 1 mm $1/e^2$ diameter. To create a spatially varying ac-Stark shift on the 3P_0 state, the 1388-nm laser is blue detuned from the $^3P_0 - ^3D_1$ transition, as shown in Fig. 1(c). The counterpropagating 1388-nm laser can be configured to form either an intensity lattice (lin||lin) or a polarization gradient lattice (lin \perp lin). We have opted for the lin||lin configuration, where the minimum light shift corresponds to zero intensity of the ac-Stark shift beam [27], though both configurations yield useful cooling. We note that multiple dipole allowed transitions that connect the 3P_0 state to higher-lying excited states could be used for implementing the Sisyphus cooling, including 3S_1 and 3D_1 states [27,31]. In our experiment, we choose the $^3D_1(F = 3/2)$ state, since the 1388-nm laser is already used for detection of the $6s6p$ 3P_0 state and have experimentally verified Sisyphus cooling is also effective with the other hyperfine components $^3D_1(F = 1/2)$.

Sisyphus cooling in free space—We first demonstrate Sisyphus cooling with untrapped atoms in free space. Atoms are cooled in a 556-nm narrow-line MOT with a measured temperature of ~ 20 μ K. After turning off the 556-nm laser, we turn on both the 578-nm clock light,

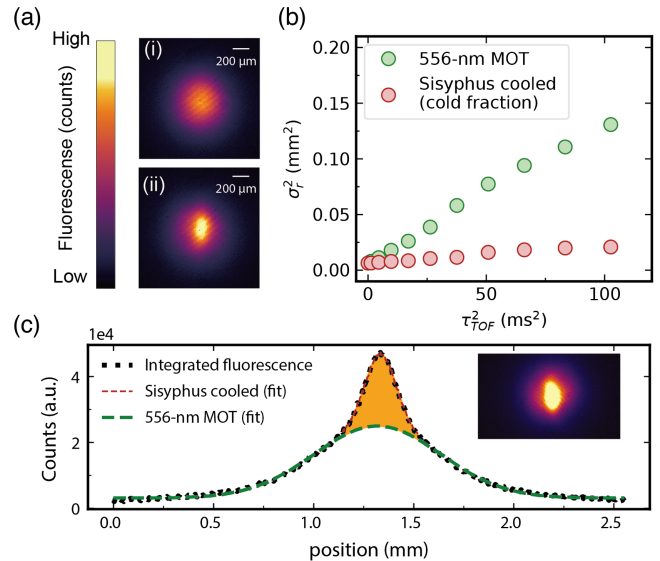


FIG. 2. Sisyphus cooling in free space. (a) Fluorescence images of the atomic sample during free expansion: (i) without and (ii) with Sisyphus cooling applied. (b) TOF trace of the 1σ radius obtained from the Gaussian fits to the horizontal, Sisyphus-cooling direction. The temperature is ~ 20 μ K for the narrow-line MOT and ~ 3 μ K for the Sisyphus-cooled fraction. (c) Integrated fluorescence profiles of the atomic sample showing Sisyphus cooling. Black points are the measured integrated fluorescence along the vertical axis. The shaded orange area and red dashed fit indicate the narrower Gaussian of the Sisyphus-cooled fraction ($\sim 20\%$). The green dashed fit line shows the broader Gaussian corresponding to the non-Sisyphus-cooled sample from the narrow-line MOT.

characterized by a Rabi frequency exceeding kilohertz, and the 1388-nm laser for 7 ms of Sisyphus cooling as the atoms also begin to fall under gravity before taking fluorescence images; see Fig. 2(a). The 578-nm clock laser needs to be spectrally narrow and frequency stable only compared to the desired excitation Rabi rate and not the clock-transition natural linewidth. We measure a time-of-flight (TOF) temperature of $\sim 3 \mu\text{K}$ for the Sisyphus-cooled fraction [see Fig. 2(b)], which is about 20% of the total atomic sample [see Fig. 2(c)]. Cooling is optimized by blue detuning the 1388-nm laser to $\Delta \simeq +50 \text{ MHz}$ from the $^3P_0 - ^3D_1$ ($F = 3/2$) transition. This corresponds to a Sisyphus potential depth of $U/h > 50 \text{ kHz}$ ($U/k_B > 2.4 \mu\text{K}$) in the 3P_0 state [27].

Adding Sisyphus cooling during the last 10 ms of the narrow-line MOT and for a further 10 ms after the MOT is extinguished, we observe enhanced loading into the magic-wavelength optical lattice by a factor of ~ 4 . This enhancement works consistently for a broad range of optical lattice trap depths, from $10 E_r$ to $100 E_r$. Here, E_r is the lattice photon recoil energy, given by $E_r = \hbar^2/(2m\lambda_{\text{latt}}^2)$, where \hbar is Planck's constant, m is the mass of ^{171}Yb , and λ_{latt} is the 759-nm lattice wavelength. We expect the above-mentioned enhancement can be improved with higher clock-light Rabi frequency, better spatial overlap of the 578-nm clock-excitation beam with the green MOT, and a deeper Sisyphus potential.

1D subrecoil Sisyphus cooling in a magic-wavelength lattice—We next demonstrate Sisyphus cooling for atoms already trapped in the 1D lattice. We note that the lattice is magic (light-shift-free) for the $^1S_0 - ^3P_0$ clock transition, used here for the initial excitation in the cooling process; see Fig. 3. We applied Sisyphus cooling along a single radial direction of the 1D lattice with the 1388-nm frequency set blue detuned $\Delta \simeq 150 \text{ MHz}$ from the $^3P_0 \rightarrow ^3D_1$ ($F = 3/2$) transition [27] and then measured the temperature using Doppler spectroscopy. Atoms are also confined in the magic-wavelength lattice with a depth of $60 E_r$. The resulting 1D temperatures are shown in Fig. 3(a) as a function of cooling time for two different excitation rates on the 578-nm clock transition. We compare cooling performance between excitation at two different Rabi frequencies on the clock transition. Stronger clock excitation ($\Omega_{578 \text{ nm}}/2\pi = 2.7 \text{ kHz}$) resulted in faster cooling, in this case corresponding to an exponential time constant of $\sim 36(5) \text{ ms}$. Because excitation on the clock transition can be the most time-consuming step in the cooling cycle, faster excitation naturally affords faster cooling. However, the higher Rabi frequency also resulted in a higher steady-state cooled temperature of $T \sim 300 \text{ nK}$. On the other hand, weaker excitation [$\Omega_{578 \text{ nm}}/2\pi = 0.760(14) \text{ kHz}$] gave a lower temperature of $T \sim 165(5) \text{ nK}$ but with a longer cooling time constant of $123(6) \text{ ms}$. Note that the final temperatures in these two clock-excitation conditions are both well below the recoil temperature (410 nK) for the

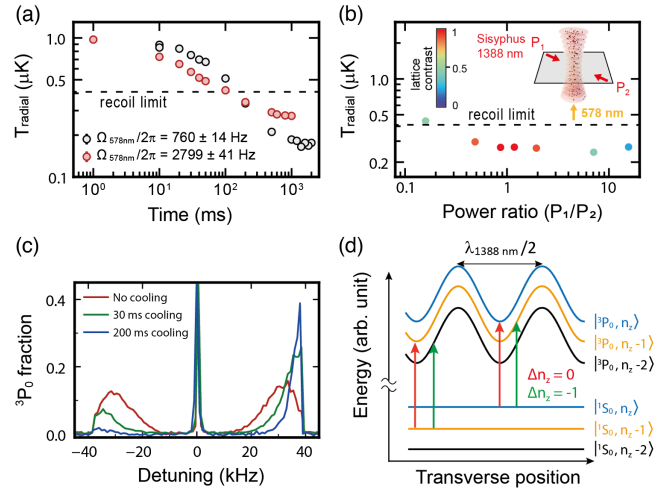


FIG. 3. Sisyphus cooling in a magic-wavelength lattice. (a) Measured radial temperature as a function of 1D Sisyphus-cooling time at $60 E_r$ with different 578-nm clock-excitation Rabi frequencies. (b) 1D Sisyphus cooling as a function of the power ratio of counterpropagating 1388-nm Sisyphus lattice laser beams for a cooling time of 500 ms with clock Rabi frequency of 2.8 kHz, where the total 1388-nm laser power remains constant. The lattice modulation of the 3P_0 energy decreases only by at most 27% for a power imbalance ratio of up to 10. (c) Longitudinal sideband spectra for no 2D Sisyphus cooling (red), 30 ms (green), and 200 ms (blue) 2D radial Sisyphus cooling, demonstrating an effective 3D cooling. (d) The spatial variation of the ac-Stark shift allows red sideband cooling by moving the lower motional state to resonance with the clock light, which is originally set to drive the carrier transition.

cascaded spontaneous decay $^3D_1 - ^3P_1 - ^1S_0$ of the cooling cycle, $k_B T_r = \hbar^2(k_{D-P}^2 + k_{P-S}^2)/2m$, where k_{D-P} (k_{P-S}) is the wavenumber corresponding to the $^3D_1 \rightarrow ^3P_1$ ($^3P_1 \rightarrow ^1S_0$) transition and k_B is the Boltzmann constant.

Our interpretation for the subrecoil temperature and the decrease of the steady-state temperature with the Rabi frequency (Ω_{clock}) is as follows. The periodic ac-Stark shift (Sisyphus potential) leads to a spatially dependent excitation profile of the clock light. With a deep Sisyphus potential ($U/h \sim \text{tens of kilohertz}$) [27], atomic motion is quantized. Away from the Sisyphus potential minimum, ground state atoms are not resonant with the clock excitation due to the ac-Stark shift of the 3P_0 state and, therefore, are decoupled from the atom-laser interaction. This creates a spatial dark region [see Fig. 1(a)], where atoms experience periods of darkness to the clock light, an effective “dark state” [32–34]. Increasing Ω_{clock} effectively increases an atom's chances of exiting the dark state. We observe that the subrecoil cooling performance is robust against power imbalance in the counterpropagating Sisyphus lattice beams. As Fig. 3(b) shows, similar temperatures are obtained with relatively large power imbalances.

3D cooling in a magic-wavelength lattice—We apply Sisyphus cooling in the plane transverse to the magic-wavelength lattice axis [27]; see Fig. 1(b). We operate the magic-wavelength lattice at a depth of $\sim 107 E_r$ and derive

atomic temperature via the axial sideband spectra; see Fig. 3(c). Without Sisyphus cooling, a noticeable red sideband amplitude reflects the atoms' population among the lattice bands with $n_z > 0$, as shown by the red curves in Fig. 3(c). The measured ratio of red and blue sideband areas give a longitudinal temperature of $\sim 9 \mu\text{K}$ [35]. After applying Sisyphus cooling for 200 ms, the blue sideband narrows, a signature of lower radial temperature [35]. In our 2D Sisyphus cooling, we consistently achieve a radial temperature near the recoil limit 410 nK. We note that the longitudinal temperature [proportional to the red sideband (RSB) amplitude] also decreases to $\sim 0.8 \mu\text{K}$, despite applying Sisyphus cooling only along the radial directions. Longitudinal cooling occurs due to a motional sideband cooling process: In some regions of the 1388-nm Sisyphus potential, the energy of the $|^3P_0, n_z = n - 1\rangle$ state is ac-Stark shifted into resonance with the unperturbed transition, satisfying the longitudinal red sideband cooling condition [12], as depicted in Fig. 3(d). Under a range of experimentally accessible magic-wavelength trap depths, we find that the red sideband cooling conditions are satisfied. For example, with the same Sisyphus potential used in the $\sim 107 E_r$ magic-wavelength lattice, we also observed a similar longitudinal temperature of $\sim 0.8 \mu\text{K}$ even when we intentionally reduced the magic-wavelength lattice depth by half to $\sim 55 E_r$.

Motional-state-selective excitation on the blue sideband—We also explore an alternative method for achieving subrecoil temperatures using the narrow clock transition to selectively excite atoms on the blue sideband ($\Delta n_z = +1$) (BSB) in a 1D optical lattice. This approach combines the techniques of light-induced evaporation [36] and cyclic cooling [22,37] and utilizes information of the radial energy distribution $E(n_r)$ encoded in the BSB spectra [35,38]; see Fig. 4(a). Our method is similar to a recent experiment of motion-selective coherent population trapping [39,40], where a higher vibration frequency of the trapped atom is selectively excited by Raman beams. Here, by adjusting the frequency of the clock laser (f_{select}) below the lattice trap corner frequency (f_{corner}), we selectively excite atoms with higher radial motional energy into the 3P_0 clock state while leaving those with lower energy in the 1S_0 state, effectively dark to the selection light; see Fig. 4(b). Radially hot atoms are cooled and quenched from the 3P_0 clock state using the Sisyphus potential.

A cooling cycle consists of the following four steps. First, using the narrow clock laser, we excite at f_{select} on the BSB; see Fig. 4(c). Second, we apply Sisyphus cooling for 1 ms with a 1388-nm laser detuning $\Delta \approx +50 \text{ MHz}$ and an optical power of $\approx 100 \mu\text{W}$ [27]. Third, using the narrow clock laser, we apply a 2 ms $^1S_0 \rightarrow ^3P_0$ adiabatic rapid passage (ARP) on the red sideband ($\Delta n_z = -1$) [41]. Fourth, we use the Sisyphus cooling again to restore population to 1S_0 . Starting with a recoil temperature limited sample, we achieved subrecoil temperatures in ten cycles,

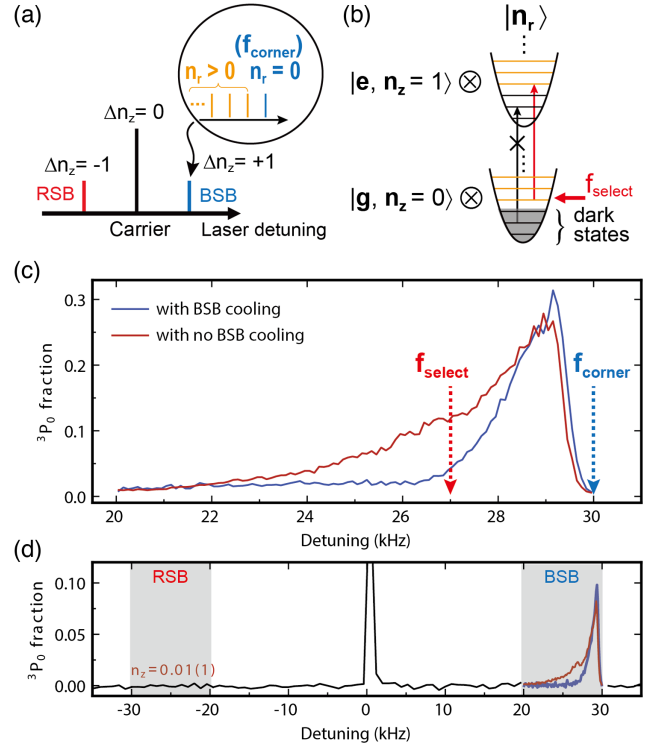


FIG. 4. Blue sideband assisted velocity selection toward subrecoil temperature. (a) Lamb-Dicke regime spectroscopy in a 1D optical lattice: The most intense line represents the carrier, where the red (blue) line represents the first-order RSB (BSB) transition. Higher radial energies smear the sidebands to the carrier. The excited radial modes ($n_r > 0$) depicted in the color orange within the BSB. (b) Two states addressed by radiation. Those with insufficient radial energy are unexcited, dark states. Those with sufficient radial energy are referred to as bright states and can be easily excited. (c) We plot the BSB before and after our BSB cooling to subrecoil temperatures. The upper edge of the BSB, referred to as f_{corner} , marks the minimum radial temperature, while f_{select} sets the threshold for dark states. (d) Longitudinal sideband spectra at $61.3(4) E_r$, both before and after the BSB cooling. RSB and BSB transitions are highlighted with shaded areas, respectively. Additional longitudinal cooling was applied via two RSB ARPs in both cases, which demonstrates the low 3D temperatures [$\bar{n}_z = 0.01(1)$] that we observed.

which lasts for a total of 81 ms. The radial temperature dropped from 451(35) to 314(37) nK and reduced the amplitude of the BSB at frequencies below f_{select} ; see Fig. 4(c). However, the atom loss was comparable to an energy filtering method (adiabatically ramping the magic-wavelength trap depth down and back up). Despite the BSB excitation, no noticeable longitudinal heating was measured [see Fig. 4(d)]; thus, we expect that atom loss was due to unwanted optical pumping to the 3P_2 metastable state. In principle, this loss can be eliminated by adding a repump laser. We note that the longitudinal cooling of the Sisyphus potential makes “continuous” BSB cooling possible. During continuous operation of the clock laser at f_{select} and the Sisyphus potential, we measure subrecoil radial temperatures and \bar{n}_z below 0.32(5).

We demonstrate Sisyphus cooling of ^{171}Yb atoms with a spatially varying ac-Stark shift on the 3P_0 state from 1388-nm laser light, which is also often used for excited clock state depumping. We enhance the loading of atoms into the magic-wavelength optical lattice and reach subrecoil temperatures with both pulsed and continuous cooling. We show 1D Sisyphus cooling to a temperature of 165(5) nK. We create a 2D Sisyphus potential in the transverse plane of the magic-wavelength optical lattice, enabling effective 3D cooling. This approach represents a straightforward modification to the typical 1D optical lattice clock architecture and could prove useful to high-performance portable clock systems. We further realize subrecoil temperatures assisted by the “energy-selective excitation” on the blue sideband that is broadened by the radial motion of the atoms.

Our cooling does not require dynamically reducing the trapping potentials. Therefore, the trap frequency remained high during the cooling process, which could allow for accelerating (runaway) evaporative cooling [42]. In addition, this method does not require a favorable elastic scattering rate, which is essential for evaporative cooling. This makes it suitable for cooling fermions, such as those used in optical lattice clocks. We expect these techniques to find applicability in other alkaline-earth(-like) atoms [18,23]. While narrow-line cooling to a few μK has been recently demonstrated in Cd [23], laser cooling in Hg and Mg are currently limited to temperatures of several tens of μK , preventing efficient lattice trap loading. Meanwhile, lattice depths at their respective magic wavelengths are also limited by available laser power, making it more challenging to achieve a deep lattice to facilitate loading without a build-up cavity. Through dressing the long-lived state with a periodic ac-Stark shift [27,31] (Hg, $6s6p^3P_0 \rightarrow 6s7s^3S_1$ at 405 nm [18]; Mg, $3s3p^3P_1 \rightarrow 3s4s^1S_0$ at 462 nm [17]), the Sisyphus-cooling method could produce deeper cooling, increasing the loading efficiency of shallow UV lattices, as compared to the cooling using the intercombination line.

Here, we have demonstrated efficient cooling without requiring high-power clock laser beams or time-varying optical or magnetic fields [43]. This may enable continuous quantum sensors to operate with high bandwidth, high signal-to-noise ratio while free from aliasing [44–47]. By controlling the illumination region of the clock light, our method, in principle, allows for site-selective cooling and imaging [48]. It could also serve as a unique quantum engineering tool for the realization of novel nonequilibrium states [49] and enabling subsystem readout during a quantum process, such as mid-circuit measurements.

These Sisyphus-cooling techniques may be applicable to (anti)hydrogen experiments [7,50]. Currently, laser cooling using pulsed narrow-linewidth Lyman- α transition light was recently demonstrated in cooling magnetically trapped antihydrogen [7]. Additionally, there has been a successful

demonstration of hydrogen beam deceleration [50]. Our work has the potential to contribute to the exploration of antihydrogen cooling schemes exploiting the dressed metastable state [19], for improved spectroscopic precision.

Acknowledgments—We acknowledge useful conversations with Tobias Bothwell. We thank Vladi Gerginov and Wesley Brand for careful reading of the manuscript and providing insightful comments. K. G. acknowledges the financial support from the United States National Science Foundation under Grant No. 2012117. This work was supported by NIST, Office of Naval Research, and National Science Foundation QLCI Grant No. 2016244.

-
- [1] Andrew D. Ludlow, Martin M. Boyd, Jun Ye, E. Peik, and P. O. Schmidt, Optical atomic clocks, *Rev. Mod. Phys.* **87**, 637 (2015).
 - [2] Immanuel Bloch, Jean Dalibard, and Sylvain Nascimbène, Quantum simulations with ultracold quantum gases, *Nat. Phys.* **8**, 267 (2012).
 - [3] T. M. Graham *et al.*, Multi-qubit entanglement and algorithms on a neutral-atom quantum computer, *Nature (London)* **604**, 457 (2022).
 - [4] Dolev Bluvstein, Harry Levine, Giulia Semeghini, Tout T. Wang, Sepehr Ebadi, Marcin Kalinowski, Alexander Keesling, Nishad Maskara, Hannes Pichler, Markus Greiner, Vladan Vuletić, and Mikhail D. Lukin, A quantum processor based on coherent transport of entangled atom arrays, *Nature (London)* **604**, 451 (2022).
 - [5] Martin Ringbauer, Michael Meth, Lukas Postler, Roman Stricker, Rainer Blatt, Philipp Schindler, and Thomas Monz, A universal qubit quantum processor with trapped ions, *Nat. Phys.* **18**, 1053 (2022).
 - [6] M. S. Safronova, D. Budker, D. DeMille, Derek F. Jackson Kimball, A. Derevianko, and C. W. Clark, Search for new physics with atoms and molecules, *Rev. Mod. Phys.* **90**, 025008 (2018).
 - [7] C. J. Baker *et al.*, Laser cooling of antihydrogen atoms, *Nature (London)* **592**, 35 (2021).
 - [8] M. D. Di Rosa, Laser-cooling molecules, *Eur. Phys. J. D* **31**, 395 (2004).
 - [9] Guo-Zhu Zhu, Debayan Mitra, Benjamin L. Augenbraun, Claire E. Dickerson, Michael J. Frim, Guanming Lao, Zack D. Lasner, Anastassia N. Alexandrova, Wesley C. Campbell, Justin R. Caram, John M. Doyle, and Eric R. Hudson, Functionalizing aromatic compounds with optical cycling centres, *Nat. Chem.* **14**, 995 (2022).
 - [10] Claire E. Dickerson, Han Guo, Ashley J. Shin, Benjamin L. Augenbraun, Justin R. Caram, Wesley C. Campbell, and Anastassia N. Alexandrova, Franck-condon tuning of optical cycling centers by organic functionalization, *Phys. Rev. Lett.* **126**, 123002 (2021).
 - [11] Hidetoshi Katori, V. D. Ovsiannikov, S. I. Marmo, and V. G. Palchikov, Strategies for reducing the light shift in atomic clocks, *Phys. Rev. A* **91**, 052503 (2015).
 - [12] R. C. Brown, N. B. Phillips, K. Beloy, W. F. McGrew, M. Schioppo, R. J. Fasano, G. Milani, X. Zhang, N. Hinkley,

- H. Leopardi, T. H. Yoon, D. Nicolodi, T. M. Fortier, and A. D. Ludlow, Hyperpolarizability and operational magic wavelength in an optical lattice clock, *Phys. Rev. Lett.* **119**, 253001 (2017).
- [13] Kyungtae Kim, Alexander Aepli, Tobias Bothwell, and Jun Ye, Evaluation of lattice light shift at low 10^{-19} uncertainty for a shallow lattice Sr optical clock, *Phys. Rev. Lett.* **130**, 113203 (2023).
- [14] Ivaylo S. Madjarov, Jacob P. Covey, Adam L. Shaw, Joonhee Choi, Anant Kale, Alexandre Cooper, Hannes Pichler, Vladimir Schkolnik, Jason R. Williams, and Manuel Endres, High-fidelity entanglement and detection of alkaline-earth Rydberg atoms, *Nat. Phys.* **16**, 857 (2020).
- [15] Nathan Schine, Aaron W. Young, William J. Eckner, Michael J. Martin, and Adam M. Kaufman, Long-lived Bell states in an array of optical clock qubits, *Nat. Phys.* **18**, 1067 (2022).
- [16] Peter W. Graham, Jason M. Hogan, Mark A. Kasevich, and Surjeet Rajendran, New method for gravitational wave detection with atomic sensors, *Phys. Rev. Lett.* **110**, 171102 (2013).
- [17] Nils Rehbein, T. E. Mehlstäubler, J. Keupp, K. Moldenhauer, E. M. Rasel, W. Ertmer, A. Douillet, V. Michels, S. G. Porsev, A. Derevianko, C. Froese Fischer, G. I. Tachiev, and V. G. Pal'chikov, Optical quenching of metastable magnesium, *Phys. Rev. A* **76**, 043406 (2007).
- [18] H. Hachisu, K. Miyagishi, S. G. Porsev, A. Derevianko, V. D. Ovsiannikov, V. G. Pal'chikov, M. Takamoto, and H. Katori, Trapping of neutral mercury atoms and prospects for optical lattice clocks, *Phys. Rev. Lett.* **100**, 053001 (2008).
- [19] Saijun Wu, Roger C. Brown, William D. Phillips, and J. V. Porto, Pulsed Sisyphus scheme for laser cooling of atomic (anti)hydrogen, *Phys. Rev. Lett.* **106**, 213001 (2011).
- [20] C. C. Chen, S. Bennetts, R. González Escudero, F. Schreck, and B. Pasquiou, Sisyphus optical lattice decelerator, *Phys. Rev. A* **100**, 023401 (2019).
- [21] Hidetoshi Katori, Masao Takamoto, V. G. Pal'chikov, and V. D. Ovsiannikov, Ultrastable optical clock with neutral atoms in an engineered light shift trap, *Phys. Rev. Lett.* **91**, 173005 (2003).
- [22] David E. Pritchard, Cooling neutral atoms in a magnetic trap for precision spectroscopy, *Phys. Rev. Lett.* **51**, 1336 (1983).
- [23] A. Yamaguchi, M. S. Safronova, K. Gibble, and H. Katori, Narrow-line cooling and determination of the magic wavelength of Cd, *Phys. Rev. Lett.* **123**, 113201 (2019).
- [24] B. Graner, Y. Chen, E. G. Lindahl, and B. R. Heckel, Reduced limit on the permanent electric dipole moment of ^{199}Hg , *Phys. Rev. Lett.* **116**, 161601 (2016).
- [25] J. R. Guest, N. D. Scielzo, I. Ahmad, K. Bailey, J. P. Greene, R. J. Holt, Z.-T. Lu, T. P. O'Connor, and D. H. Potterveld, Laser trapping of ^{225}Ra and ^{226}Ra with repumping by room-temperature blackbody radiation, *Phys. Rev. Lett.* **98**, 093001 (2007).
- [26] W. F. McGrew, X. Zhang, R. J. Fasano, S. A. Schäffer, K. Beloy, D. Nicolodi, R. C. Brown, N. Hinkley, G. Milani, M. Schioppo, T. H. Yoon, and A. D. Ludlow, Atomic clock performance enabling geodesy below the centimetre level, *Nature (London)* **564**, 87 (2018).
- [27] See Supplemental Material at <http://link.aps.org/supplemental/10.1103/PhysRevLett.133.053401> for details on higher-lying excited-state selection for inducing the Sisyphus lattice, 1388-nm Sisyphus beam configurations, and further analysis of the ac-Stark shift, which includes Refs. [28–30].
- [28] K. Beloy, J. A. Sherman, N. D. Lemke, N. Hinkley, C. W. Oates, and A. D. Ludlow, Determination of the $5d6s\ ^3D_1$ state lifetime and blackbody-radiation clock shift in Yb, *Phys. Rev. A* **86**, 051404(R) (2012).
- [29] R. Hobson, W. Bowden, A. Vianello, I. R. Hill, and Patrick Gill, Midinfrared magneto-optical trap of metastable strontium for an optical lattice clock, *Phys. Rev. A* **101**, 013420 (2020).
- [30] Tomoya Akatsuka, Koji Hashiguchi, Tadahiro Takahashi, Noriaki Ohmae, Masao Takamoto, and Hidetoshi Katori, Three-stage laser cooling of Sr atoms using the $5s5p\ ^3P_2$ metastable state below doppler temperatures, *Phys. Rev. A* **103**, 023331 (2021).
- [31] In a clock-line-mediated Sisyphus-cooling scheme employing the 3D_1 as the higher-lying excited state, if no repumper is applied, atoms fall out of the cooling cycle once they decay to the 3P_2 dark state (branching ratio $\sim 1\%$ for $^3D_1 \rightarrow ^3P_2$). However, only a few cooling cycles are required to transition from the initial temperatures of 3P_1 Doppler cooling down to the recoil limit.
- [32] R. Dum, P. Marte, T. Pellizzari, and P. Zoller, Laser cooling to a single quantum state in a trap, *Phys. Rev. Lett.* **73**, 2829 (1994).
- [33] R. Dum, Cooling using velocity or mode selection for alkali-metal atoms, *Phys. Rev. A* **54**, 3299 (1996).
- [34] G. Morigi, J. I. Cirac, K. Ellinger, and P. Zoller, Laser cooling of trapped atoms to the ground state: A dark state in position space, *Phys. Rev. A* **57**, 2909 (1998).
- [35] S. Blatt, J. W. Thomsen, G. K. Campbell, A. D. Ludlow, M. D. Swallows, M. J. Martin, M. M. Boyd, and J. Ye, Rabi spectroscopy and excitation inhomogeneity in a one-dimensional optical lattice clock, *Phys. Rev. A* **80**, 052703 (2009).
- [36] I. D. Setija, H. G. C. Werij, O. J. Luiten, M. W. Reynolds, T. W. Hijmans, and J. T. M. Walraven, Optical cooling of atomic hydrogen in a magnetic trap, *Phys. Rev. Lett.* **70**, 2257 (1993).
- [37] D. E. Pritchard, K. Helmerson, V. S. Bagnato, G. P. Lafyatis, and A. G. Martin, Optical pumping in translation space, in *Laser Spectroscopy VIII*, Springer Series in Optical Sciences, edited by Willy Persson and Sune Svanberg (Springer, Berlin, 1987), pp. 68–72.
- [38] K. Beloy, W. F. McGrew, X. Zhang, D. Nicolodi, R. J. Fasano, Y. S. Hassan, R. C. Brown, and A. D. Ludlow, Modeling motional energy spectra and lattice light shifts in optical lattice clocks, *Phys. Rev. A* **101**, 053416 (2020).
- [39] Hyun Gyung Lee, Sooyoung Park, Meung Ho Seo, and D. Cho, Motion-selective coherent population trapping for subrecoil cooling of optically trapped atoms outside the Lamb-Dicke regime, *Phys. Rev. A* **106**, 023324 (2022).
- [40] Sooyoung Park, Meung Ho Seo, Ryun Ah Kim, and D. Cho, Motion-selective coherent population trapping by Raman sideband cooling along two paths in a Λ configuration, *Phys. Rev. A* **106**, 023323 (2022).
- [41] J. L. Siegel, W. F. McGrew, Y. S. Hassan, C.-C. Chen, K. Beloy, T. Grogan, X. Zhang, and A. D. Ludlow,

- Excited-band coherent delocalization for improved optical lattice clock performance, *Phys. Rev. Lett.* **132**, 133201 (2024).
- [42] Chen-Lung Hung, Xibo Zhang, Nathan Gemelke, and Cheng Chin, Accelerating evaporative cooling of atoms into Bose-Einstein condensation in optical traps, *Phys. Rev. A* **78**, 011604(R) (2008).
- [43] X. Zhang, K. Beloy, Y. S. Hassan, W. F. McGrew, C.-C. Chen, J. L. Siegel, T. Grogan, and A. D. Ludlow, Subrecoil clock-transition laser cooling enabling shallow optical lattice clocks, *Phys. Rev. Lett.* **129**, 113202 (2022).
- [44] J. M. Kwolek and A. T. Black, Continuous sub-Doppler-cooled atomic beam interferometer for inertial sensing, *Phys. Rev. Appl.* **17**, 024061 (2022).
- [45] Judith Olson, Richard W. Fox, Tara M. Fortier, Todd F. Sheerin, Roger C. Brown, Holly Leopardi, Richard E. Stoner, Chris W. Oates, and Andrew D. Ludlow, Ramsey-Bordé matter-wave interferometry for laser frequency stabilization at 10^{-16} frequency instability and below, *Phys. Rev. Lett.* **123**, 073202 (2019).
- [46] Hidetoshi Katori, Longitudinal Ramsey spectroscopy of atoms for continuous operation of optical clocks, *Appl. Phys. Express* **14**, 072006 (2021).
- [47] Ryoto Takeuchi, Hayaki Chiba, Shoichi Okaba, Masao Takamoto, Shigenori Tsuji, and Hidetoshi Katori, Continuous outcoupling of ultracold strontium atoms combining three different traps, *Appl. Phys. Express* **16**, 042003 (2023).
- [48] Jacob P. Covey, Ivaylo S. Madjarov, Alexandre Cooper, and Manuel Endres, 2000-times repeated imaging of strontium atoms in clock-magic tweezer arrays, *Phys. Rev. Lett.* **122**, 173201 (2019).
- [49] Christie S. Chiu, Geoffrey Ji, Anton Mazurenko, Daniel Greif, and Markus Greiner, Quantum state engineering of a Hubbard system with ultracold fermions, *Phys. Rev. Lett.* **120**, 243201 (2018).
- [50] S. F. Cooper, C. Rasor, R. G. Bullis, A. D. Brandt, and D. C. Yost, Optical deceleration of atomic hydrogen, *New J. Phys.* **25**, 093038 (2023).